

Remarkable stabilisation of the intercalated smectic phases of nonsymmetric dimers by *tert*-butyl groups

Rebecca Walker, Damian Pociecha, Camilla Faidutti, Eva Perkovic, John M. D. Storey, Ewa Gorecka & Corrie T. Imrie

To cite this article: Rebecca Walker, Damian Pociecha, Camilla Faidutti, Eva Perkovic, John M. D. Storey, Ewa Gorecka & Corrie T. Imrie (2022) Remarkable stabilisation of the intercalated smectic phases of nonsymmetric dimers by *tert*-butyl groups, *Liquid Crystals*, 49:7-9, 969-981, DOI: [10.1080/02678292.2022.2055797](https://doi.org/10.1080/02678292.2022.2055797)

To link to this article: <https://doi.org/10.1080/02678292.2022.2055797>



© 2022 The Author(s). Published by Informa UK Limited, trading as Taylor & Francis Group.



Published online: 18 Apr 2022.



[Submit your article to this journal](#)



Article views: 624



[View related articles](#)







[View Crossmark data](#)



Citing articles: 5 [View citing articles](#)

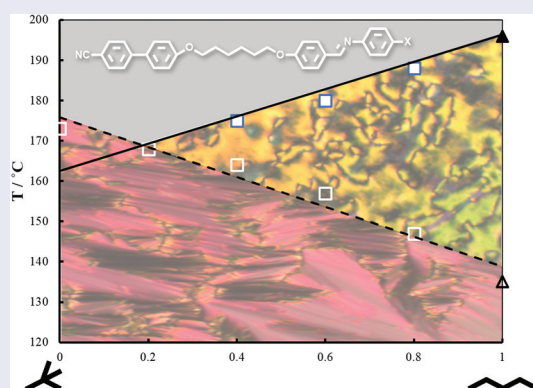
Remarkable stabilisation of the intercalated smectic phases of nonsymmetric dimers by *tert*-butyl groups

Rebecca Walker ^a, Damian Pocięcha ^b, Camilla Faidutti^a, Eva Perkovic^a, John M. D. Storey^a, Ewa Gorecka ^b and Corrie T. Imrie ^a

^aDepartment of Chemistry, Meston Building, King's College, University of Aberdeen, Aberdeen, UK; ^bDepartment of Chemistry, University of Warsaw, Warsaw, Poland

ABSTRACT

The synthesis and characterisation of two groups of nonsymmetric dimers, the 1-(4-cyanobiphenyl-4'-yloxy)- ω -(4-butyl, 4-(1-methylpropyl) or 4-*t*-butylanilinebenzylidene-4'-oxy)alkanes, and the 1-(4-cyanobiphenyl-4'-yl)- ω -(4-butyl, 4-(1-methylpropyl) or 4-*t*-butylanilinebenzylidene-4'-oxy)alkanes, are reported. The length and parity of the flexible spacer is varied. The *tert*-butyl homologues show higher melting points than the corresponding *sec*-butyl or *n*-butyl substituted dimers, suggesting that chain branching improves packing efficiency within the crystalline structure. The branched chain homologues have a stronger tendency to exhibit smectic phases than the *n*-butyl-substituted dimers, and for longer spacers are exclusively smectic. A comparison of the nematic-isotropic transition temperatures (T_{NI}) for dimers containing the different terminal chains is possible for one set of materials, and reveals a large reduction in T_{NI} on passing from the *n*-butyl to *sec*-butyl-substituted, but a much smaller decrease on changing *sec*-butyl for *tert*-butyl. A different trend is observed for the smectic A-isotropic transition temperatures for which the *tert*-butyl substituted dimers show a higher value than the corresponding *sec*-butyl homologue, and only marginally lower than that of the *n*-butyl-substituted dimer. This surprising behaviour is interpreted in terms of the ability of the *tert*-butyl group to pack more efficiently into the intercalated smectic A phase as the spacer length increases.



ARTICLE HISTORY

Received 24 October 2021



Keywords

Intercalation; branched chain; smectic phases; twist-bend

Introduction

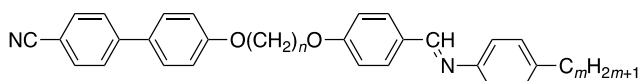
Liquid crystalline dimers consist of molecules containing two mesogenic units linked *via* a flexible spacer, most commonly an alkyl chain [1,2]. In recent years, there has been a dramatic resurgence of interest in this class of materials arising first from the observation of the twist-bend nematic phase for dimers containing an odd-membered spacer (see, e.g. [3–25]), and even more recently from the discovery

of the twist-bend smectic phases [26–28]. Prior to this, liquid crystal dimers had been the focus of considerable research interest following the discovery of the intercalated smectic phases for nonsymmetric dimers, in which the two mesogenic units differ in structure [29–31]. The intercalated smectic phases were first observed for members of the 1-(4-cyanobiphenyl-4'-yloxy)- ω -(4-alkylanilinebenzylidene-4'-oxy)alkanes [29].

CONTACT Corrie T. Imrie  c.t.imrie@abdn.ac.uk  Department of Chemistry, Meston Building, King's College, University of Aberdeen, Aberdeen AB24 3UE, UK

© 2022 The Author(s). Published by Informa UK Limited, trading as Taylor & Francis Group.

This is an Open Access article distributed under the terms of the Creative Commons Attribution-NonCommercial-NoDerivatives License (<http://creativecommons.org/licenses/by-nc-nd/4.0/>), which permits non-commercial re-use, distribution, and reproduction in any medium, provided the original work is properly cited, and is not altered, transformed, or built upon in any way.



The acronym used to refer to this family of dimers is $\text{CBO}n\text{O}.m$ where CB stands for the cyanobiphenyl unit, O for the ether linkages, n for the number of methylene units in the spacer, “.” for the benzylideneaniline moiety and m is the number of carbon atoms in the terminal alkyl chain. The discovery of the intercalated smectic phases arose from the observation of unprecedented smectic behaviour on varying the terminal chain length in the $\text{CBO}6\text{O}.m$ series [29]. Specifically, the first eleven members ($m = 0-10$) were found to show an enantiotropic nematic phase, and in addition, smectic phases were observed for $m = 0-6$ and 10. The smectic A – nematic transition temperature, T_{SmAN} , increased over the first three members and subsequently fell for $m = 3-6$. No smectic behaviour was observed for $m = 7-9$ but reappeared for $m = 10$, which showed the highest value of T_{SmAN} of the series. This behaviour was hugely surprising, and in marked contrast to that seen for conventional low molar mass liquid crystals comprising molecules containing a single mesogenic unit for which T_{SmAN} normally increases on increasing the length of a terminal alkyl chain. This novel behaviour was accounted for in terms of how the structure of the SmA phase changed as m was varied for the $\text{CBO}6\text{O}.m$ series.

For early members of the series the ratio of the layer thickness, d , to the molecular length, l , d/l was about 0.5 whereas for $m = 10$, $d/l = 1.8$. The latter value indicated an interdigitated arrangement of the molecules stabilised by the electrostatic interaction between the polar and polarizable cyanobiphenyl units, and the smectic phase resulted from the molecular inhomogeneity arising from the long terminal alkyl chains, see Figure 1. For the early members of the series, $d/l \approx 0.5$ was interpreted in terms of the formation of an intercalated smectic A phase, in which differing parts of the molecule overlap, see Figure 1. The possibility that the dimers formed horse-shoe conformations and hence, $d/l \approx 0.5$ was ruled out as being energetically unfavourable. The driving force for the formation of the intercalated arrangement has been attributed to a specific favourable interaction between the unlike mesogenic units, suggested to be an electrostatic quadrupolar interaction between groups having quadrupole moments of opposite signs [32]. The ability to accommodate the terminal chain in the intercalated arrangement is determined by the length of the spacer. The absence of smectic behaviour for $m = 7-9$ reflects a competition between two incompatible structures, neither of which wins, and hence, the nematic phase is observed rather than the monolayer smectic A phase (Figure 1). The study of the $\text{CBO}n\text{O}.m$ family of dimers not only revealed the intercalated smectic A phase but

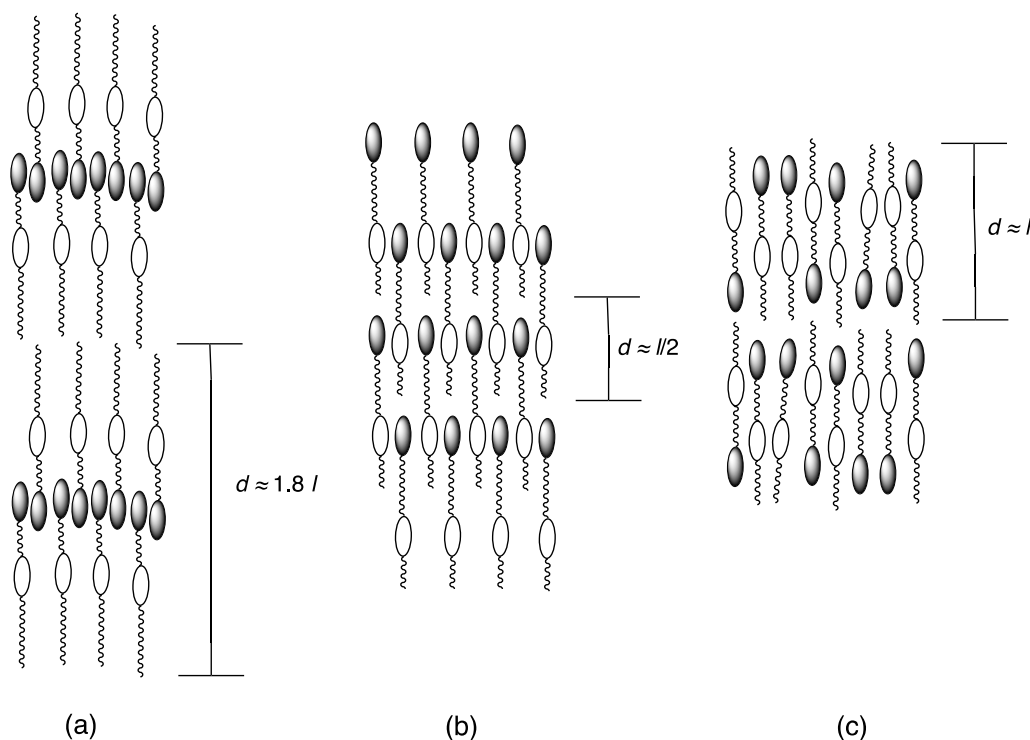


Figure 1. Sketches of the molecular organisation within (a) the interdigitated, (b) the intercalated and (c) the monolayer smectic A phases composed of nonsymmetric liquid crystal dimers: d denotes the layer spacing, and l the molecular length.

also the intercalated smectic C and I phases, and the intercalated crystal B and J phases [31]. Moreover, the intercalated smectic phases have been observed not only for dimers [33] but also for higher oligomers including trimers [34,35] and tetramers [36]. It should also be noted that the tendency of nonsymmetric dimers to form intercalated packing arrangements may play an important role in the formation of the twist-bend nematic phase [37–47].

The proposed structure of the intercalated smectic phase in which unlike molecular fragments overlap has now been widely accepted in terms of accounting for d/l ratios of much less than one for smectic phases exhibited by dimers and higher oligomers [48]. There remain, however, a number of unresolved issues with the intercalated structure and the nature of the driving force for its formation. A notable example is CBO12O.2, which exhibits an intercalated smectic A phase although the significant mismatch in length between the spacer and terminal chain would suggest that the structure will contain a considerable concentration of voids [31]. It has also been shown that mixtures of symmetric dimers such as 2.O2O.2 and CBO10OCB exhibit induced intercalated smectic A phases [31]. It is very difficult to visualise how these symmetric dimers containing very different spacer lengths can pack efficiently into an intercalated arrangement while maximising the interactions between the unlike mesogenic units. In order to investigate the nature of these intercalated phases further, and in particular to address the question of how do dissimilar fragments pack within the intercalated structure, here we report the synthesis and characterisation of two groups of nonsymmetric dimers in which the length of the spacer and steric bulk of the terminal chain are varied, see Figure 2. In both groups of materials, the terminal

substituent is either a butyl chain ($X=4$), or the isomeric *sec*-butyl ($X=s4$) and *tert*-butyl groups ($X=t4$). In the CBO n O.X dimers, the spacer has been varied to consider both the effects of length and parity on phase behaviour (Figure 2), and these are directly comparable to the CBO n O. m dimers published previously [29,31].

In the second set of materials discussed, CB n O.X, the spacer is now linked to the cyanobiphenyl unit using a methylene group and for even values of n , this endows the molecular curvature required for twist-bend liquid crystal phases to be observed as shown by the CB6O. m [47] and CB6O.O m [45] series. The branched materials will allow us to study how the steric bulk of the terminal chain affects the stability of such phases as well as the intercalated smectic phases.

Experimental

The synthesis of the diether-linked CBO n O.X dimer series followed the steps outlined in Scheme 1. The 4-{4-[(ω -bromoalkyl)oxy]phenyl}benzonitriles (1) were prepared according to a procedure described by Crivello *et al.*, [49] and the aldehyde (2) was formed by a Williamson ether synthesis. This was subsequently combined with the relevant n , *sec*- or *tert*-butyl aniline to form the desired Schiff's base (3).

The synthesis of the CB n O.X series followed the procedure outlined in Scheme 2. Noncommercial acid chlorides (4) were prepared by reacting the corresponding bromoalkanoic acid with thionyl chloride. Compounds (5)–(8) were prepared as reported previously [49]. The 1-(4-cyanobiphenyl-4'-yl)- ω -(4-formylphenyl-4'-oxy)alkanes ($n=5, 6, 8, 10$) (8) were then combined with n -, *sec*- or *tert*-butylaniline to form the desired Schiff base (9).

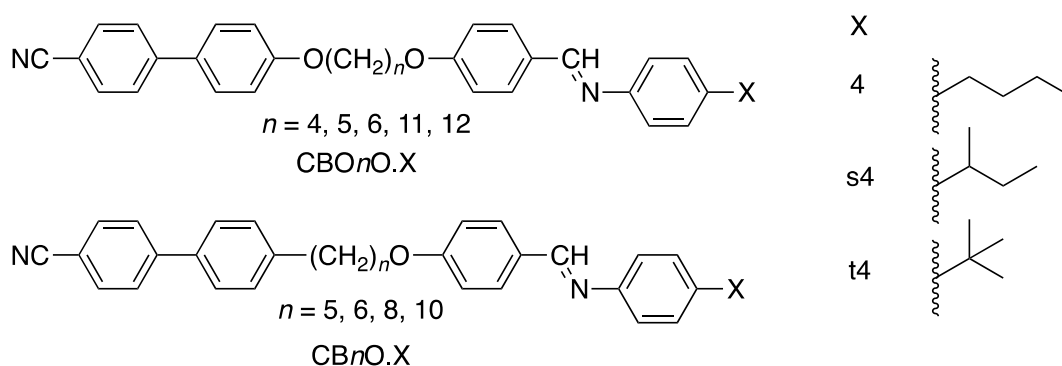
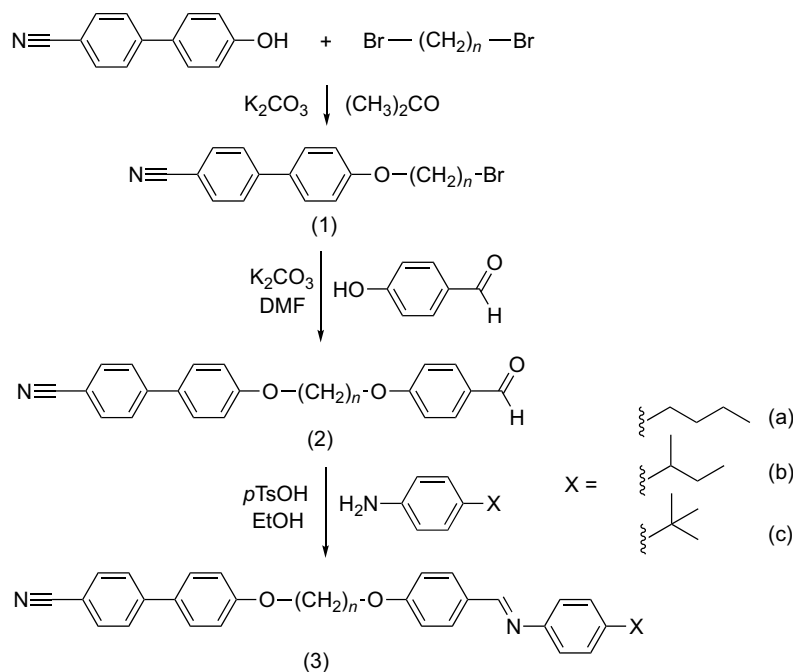


Figure 2. The nonsymmetric dimers reported here and the acronyms used to refer to them.



Scheme 1. Synthesis of the CBO n O.X dimers, where $n = 4, 5, 6, 11$ or 12 and $xX = n-, sec-$ or $tert-$ butyl.

For full synthetic procedures and analytical data, see ESI.

Results

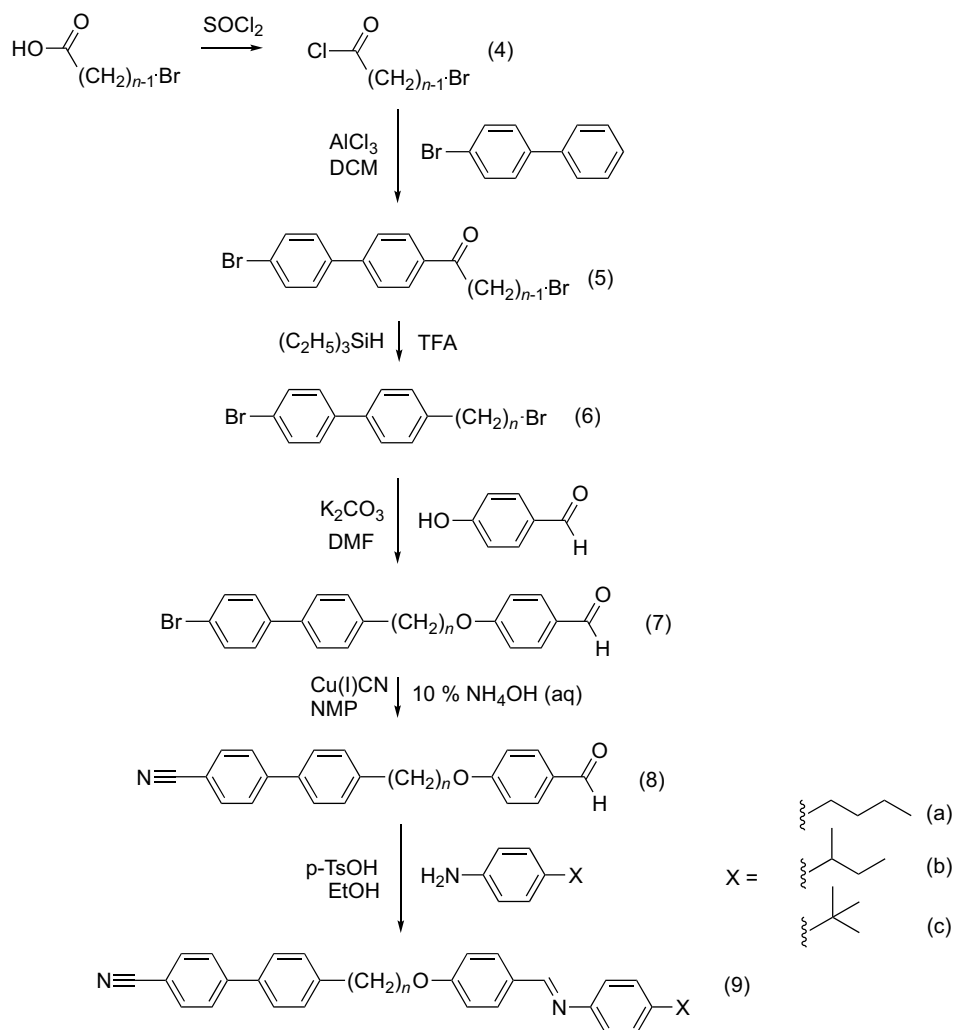
CBO n O.X series

The transitional properties of the CBO n O.X dimers are listed in Table 1. Conventional nematic phases were assigned on the basis of the observation of characteristic schlieren textures when viewed through the polarised light optical microscope containing two- and four-point brush defects and which flashed on the application of mechanical stress, see Figure 3. CBO4O.4 shows an enantiotropic nematic phase and on extensive supercooling focal conic fans developed in coexistence with regions of homeotropic alignment indicative of a smectic A phase, see Figure 3. The transition temperatures for CBO4O.4 are in excellent agreement with those published previously [31]. The X-ray diffraction pattern of the nematic phase shown by CBO4O.4 shows diffuse wide- and small-angle signals with the latter centred at about 19.1 Å. This corresponds to approximately half the molecular length and indicates a locally intercalated arrangement of the molecules. The monotropic nature of the SmA phase precluded its characterisation using X-ray diffraction, although it seems wholly reasonable to assume that this will have an intercalated structure.

CBO4O.s4 exhibited only an enantiotropic nematic phase whereas CBO4O.t4 did not exhibit liquid crystalline behaviour.

CBO5O.4 also showed an enantiotropic nematic phase and on cooling a twist-bend nematic, N_{TB} , phase [47], and the transition temperatures are in excellent agreement with literature values, although the N_{TB} phase had previously been assigned as a SmA phase [31]. CBO5O.s4 exhibited a monotropic nematic phase. On cooling this, a jagged focal conic fan texture was seen fleetingly prior to crystallisation, and this unknown smectic phase has been denoted SmX₂, see Figure 4. The monotropic nature of this phase precluded its further study using X-ray diffraction. CBO5O.t4 did not exhibit liquid crystalline behaviour.

CBO6O.4 shows a sequence of four liquid crystal phases: nematic, smectic A, hexatic smectic B (HexB) and soft crystal E. The smectic A phase was identified on the basis of the observation of coexisting regions of focal-conic fans and homeotropic alignment. On cooling into the HexB phase, the fans became smoother at the transition and less well-defined, and at the transition to the E phase a scratch-like pattern developed across their backs, see Figure 5. In the nematic phase, the X-ray pattern consists of only diffuse wide- and small-angle signals reflecting the liquid-like ordering of the molecules. The small-angle signal in the nematic phase is very



Scheme 2. Synthesis of the $CBnO.X$ dimers, where $n = 5, 6, 8$ or 10 , and $X = n$ -*sec*- or *tert*-butyl.

Table 1. The transition temperatures and associated scaled entropy changes, $\Delta S/R$, for the $CBnO.X$ series.

Dimer	$T_{Cr}/^{\circ}C$ ($\Delta S/R$)	$T_{EHxB}/^{\circ}C$ $T_{JSmI}/^{\circ}C$ † ($\Delta S/R$)	$T_{HexBSmA}/^{\circ}C$ $T_{SmISmC}/^{\circ}C$ ‡ ($\Delta S/R$)	$T_{SmCSmA}/^{\circ}C$ ($\Delta S/R$)	$T_{SmAN}/^{\circ}C$ $T_{SmX2N}/^{\circ}C$ † ($\Delta S/R$)	$T_{NTBN}/^{\circ}C$ ($\Delta S/R$)	$T_{NI}/^{\circ}C$ $T_{SmAl}/^{\circ}C$ ‡ ($\Delta S/R$)
CBO4O.4	148 (10.09)				98 ^a -		224 (1.45)
CBO4O.s4	181 (10.27)						188 (0.74)
CBO4O.t4	227 (13.98)						
CBO5O.4	108 (11.37)					73 ^b (0.004)	150 (0.50)
CBO5O.s4	136 (13.45)				72 ^{†,a} -		94 ^b (0.11)
CBO5O.t4	168 (11.64)						
CBO6O.4	111 (11.11)	89 ^b (1.19)	99 ^b (0.92)		139 (0.22)		199 (1.63)
CBO6O.s4	158 (9.05)				144 ^b (1.03)		166 (1.05)
CBO6O.t4	189 (12.90)						172 ^{†,a}
CBO11O.4	95 (13.84)	66 [¶] (0.62)	98 [§] (0.91)	112 (0.03)	142 (0.79)		152 (0.88)
CBO11O.s4	91 (11.21)	63 ^{¶,b} (0.92)	78 ^{§,b} (0.66)	109 ^a -			120 ^{‡,b} (2.70)
CBO11O.t4	141 (12.40)	73 ^{¶,a} -	80 ^{§,a} -	120 ^b (0.02)			132 ^{‡,b} (3.32)
CBO12O.4	112 (10.43)		112 (1.03)				159 [‡] (3.48)
CBO12O.s4	136 (14.34)						142 [‡] (4.23)
CBO12O.t4	159 (15.15)						148 [‡] (4.46)

^aTemperature obtained using POM.

^bData obtained from DSC cooling trace.

diffuse and centered at around 18 Å. The small-angle signal becomes sharp in the SmA phase while the wide-angle peak remains broad indicating a liquid-

like arrangement of the molecules within the layers, see Figure 5. The layer spacing, d , in the smectic A phase is 18.0 Å and approximately half the

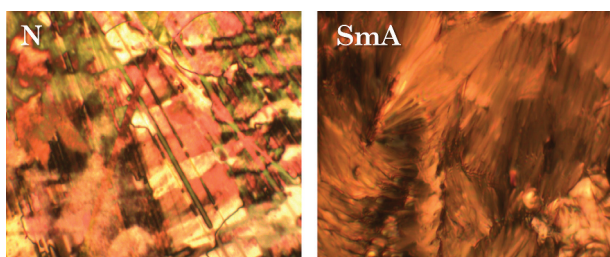


Figure 3. (Colour online) The textures obtained using the polarised light optical microscope for CBO40.4 in (left) the nematic, and (right) the smectic A phase.

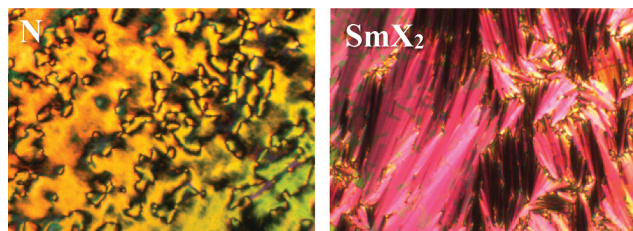


Figure 4. (Colour online) The textures obtained using the polarised optical microscope for CBO50.s4 in (left) the nematic, and (right) the smectic X_2 phase.

molecular length, l , of CBO60.4 estimated to be 33.4 Å, indicating an intercalated arrangement of the molecules. The increased in-plane order of the HexB phase is evident in the narrowing of the wide-angle signal in the X-ray diffraction pattern; the presence of several sharp signals in the X-ray pattern of the E phase indicates a highly ordered structure consistent with the phase assignment, see Figure 5. The layer spacings measured in the HexB and

E phases are 18.0 Å and 18.3 Å, respectively, with associated d/l ratios of 0.54 and 0.55, respectively, showing that the intercalated arrangement of the molecules persists in these higher ordered phases. The monotropic E and HexB phases were not identified in the previous study, but otherwise the transition temperatures are in excellent agreement [29]. CBO60.s4 exhibits only N and SmA phases, while CBO60.t4 cools directly from the isotropic phase into the SmA phase.

CBO110.4 shows a rich smectic polymorphism, having the phase sequence on cooling: I-N-SmA-SmC-SmI-J-Cr. A characteristic schlieren texture was observed in the nematic phase, which on cooling became largely homeotropic with small regions of focal conic fans indicating a SmA phase, see Figure 6. The X-ray pattern of the smectic A phase contained a sharp low angle signal and a broad wide-angle signal. On cooling, the homeotropic regions developed a weakly birefringent schlieren texture characteristic of a SmC phase, and the X-ray diffraction pattern consisted of a sharp low angle and diffuse wide-angle signal reflecting the liquid-like arrangement of the molecules within the smectic layers. On cooling the smectic C phase, the schlieren texture becomes notably brighter and somewhat less well-defined, see Figure 6. The wide-angle reflection in the X-ray diffraction pattern narrows and splits, indicating a tilted hexatic phase. For an aligned sample, the pattern shows one of the wide-angle peaks is in an equatorial position with respect to the small-angle signals, indicating that the molecules are tilted towards nearest neighbours in the local in-plane hexagons, and hence the phase has been assigned as a SmI phase. On cooling the SmI

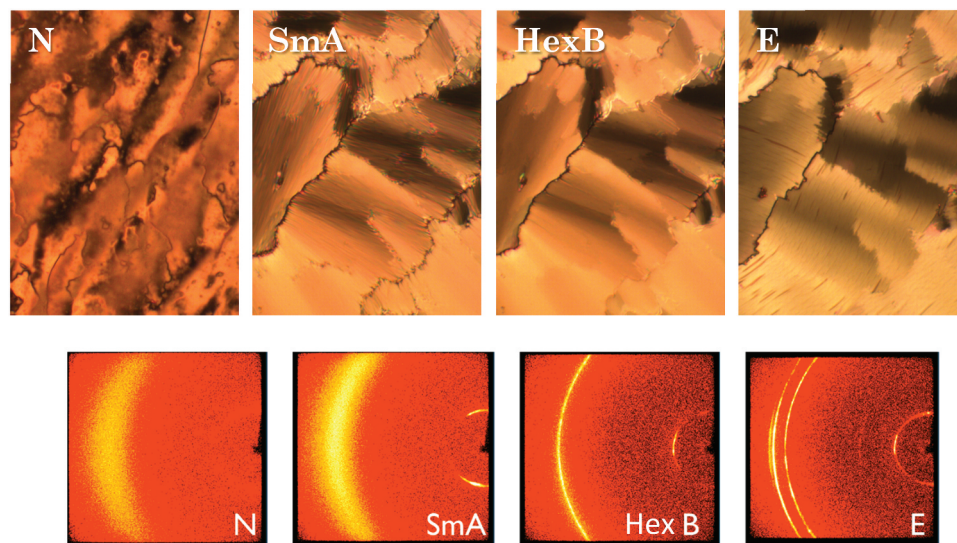


Figure 5. (Colour online) The textures obtained using the polarised light optical microscope and the corresponding X-ray diffraction patterns for CBO60.4 in (from left to right) the nematic, the smectic A, hexatic B and soft crystal E phases.

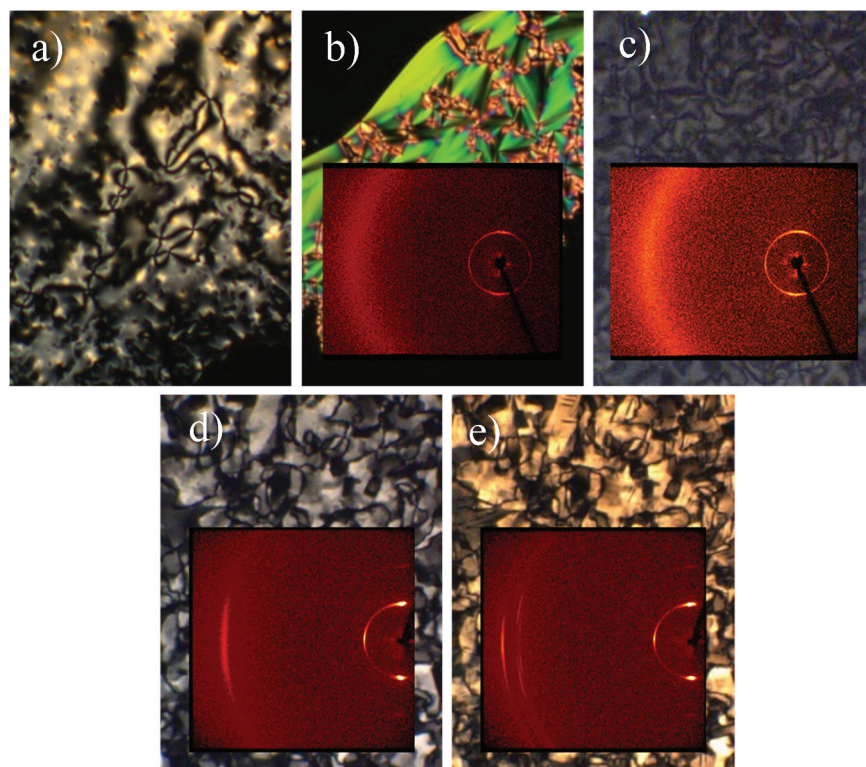


Figure 6. (Colour online) The textures obtained using the polarised optical microscope and the corresponding X-ray diffraction patterns for CBO110.4 in (a) the nematic, (b) the smectic A, (c) smectic C, (d) smectic I and (e) soft crystal J phases.

Table 2. Layer spacings, d , and ratio of layer spacing to molecular length, l , d/l , for the CBO110.X and CBO120.X series.

Dimer	Phase	$d/\text{\AA}$	d/l
CBO110.4	SmA	21.0	0.58
CBO110.4	SmC	20.8	0.58
CBO110.4	SmI	21.2	0.59
CBO110.4	J	21.1	0.59
CBO110.s4	SmA	20.6	0.60
CBO110.t4	SmA	20.7	0.63
CBO120.4	SmA	21.9	0.55
CBO120.4	HexB	22.2	0.56
CBO120.s4	SmA	21.5	0.56
CBO120.t4	SmA	21.5	0.59

phase, scratch-like defects appear on the texture and the birefringence changes. These changes are accompanied by a splitting of the wide-angle signal into a number of sharp peaks in the X-ray diffraction pattern suggesting this to be a crystal J phase. The layer spacings and the d/l ratios measured in each of the phases are listed in Table 2, and in each an intercalated arrangement of the molecules is evident. We also note that the position of the diffuse signal in the low angle region for the nematic phase is centred at around 21 Å suggesting a locally intercalated arrangement of the molecules. CBO110.s4 and CBO110.t4 show the same sequence of smectic phases but do not exhibit a nematic phase and instead show SmA-I isotropic

transitions. The phase assignments were based on the observation of similar optical textures and X-ray diffraction patterns as described for CBO110.4. The layer thicknesses measured in the SmA phase shown by CBO11.s4 and CBO110.t4 are also listed in Table 2 and these reveal intercalated arrangements.

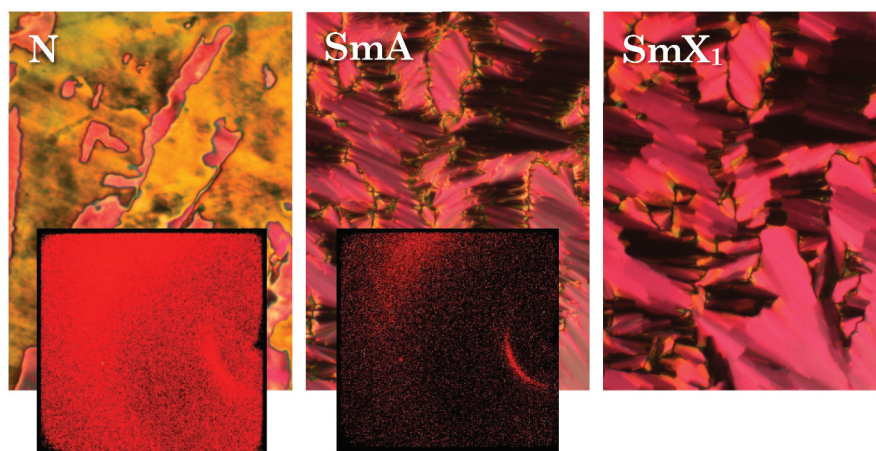
CBO120.4, CBO120.s4 and CBO120.t4 exhibit SmA-I transitions, and CBO120.4 also shows the hexatic B phase. These phases were identified on the basis of optical textures and the associated X-ray diffraction patterns, see Figure S1, and as described earlier for other homologues. The layer spacings for each CBO120.X dimer measured using X-ray diffraction are listed in Table 2, and again reveal in each case an intercalated arrangement of the molecules.

CB n O.X series

The transitional properties of the CB n O.X series are listed in Table 3. CB5O.4 shows an enantiotropic nematic phase and two monotropic smectic phases, see Figure 7. The X-ray pattern of the nematic phase consisted of diffuse peaks in the wide- and small-angle regions. On cooling the uniform texture of the nematic phase, a focal conic fan texture appears and the small-

Table 3. The transition temperatures and associated scaled entropy changes, $\Delta S/R$, for the $CBnO.X$ series.

Dimer	$T_{Cr}/^{\circ}C$ ($\Delta S/R$)	$T_{X4}/^{\circ}C$ ¶ ($\Delta S/R$)	T_{SmX5-} / $^{\circ}C$	$T_{SmX3-}/^{\circ}C$ ($\Delta S/R$)	$T_{SmC-}/^{\circ}C$ † ($\Delta S/R$)	$T_{SmX1SmA}$ / $^{\circ}C$ ($\Delta S/R$)	$T_{SmAN}/^{\circ}C$ ($\Delta S/R$)	$T_{NTBN}/^{\circ}C$ ($\Delta S/R$)	$T_{NI}/^{\circ}C$ $T_{SmC}/^{\circ}C$ ‡ ($\Delta S/R$)
CB5O.4	123 (4.95)					80 ^a - 109 ^a -	99 ^a -		204 (1.74)
CB5O.s4	143 (6.37)								167 (1.30)
CB5O.t4	204 (12.90)								160 ^a
CB6O.4	103 (9.11)							75 ^b (0.14)	115 (0.32)
CB6O.s4	104 (29.08)								
CB6O.t4	154 (23.96)								
CB8O.4	84 (15.47)	25 ^b (0.56)		70 ^b (0.73)	85 ^b (1.28)			87 ^a -	127 (0.39)
CB8O.s4	102 (15.52)	58 ^b (1.46)		64 ^b (1.01)					82 ^{‡,b} (2.80)
CB8O.t4	130 (8.99)								
CB10O.4	86 (14.09)	28 ^b (0.58)		75 ^b (0.99)	101 ^b (1.28)				129 (0.70)
CB10O.s4	83 (5.72)	36 ^b (1.41) ^c	63 ^b	67 ^b (0.92)					94 [‡] (2.64)
CB10O.t4	128 (6.17)								105 ^{‡,a} -

^aTemperature obtained using POM.^bData obtained from DSC cooling trace.^cCombined value for SmX_4 - SmX_5 - SmX_3 transition.**Figure 7.** (Colour online) The textures obtained using the polarised optical microscope and the corresponding X-ray diffraction patterns for CB5O.4 in (a) the nematic, (b) the smectic A and (c) smectic X_1 phases.

angle diffraction signal narrows whereas the wide-angle peak remains diffuse. This is indicative of a transition to the smectic A phase, and the diffraction patterns suggest an intercalated structure. On further cooling, the fans become rather blocky and truncated, and the texture is smoother. This is not a characteristic texture for the purposes of phase identification, and crystallisation precluded the study of the phase using X-ray diffraction. The phase has been arbitrarily designated the SmX_1 phase. CB5O.s4 also exhibits an enantiotropic nematic phase and on cooling, forms the SmX_1 phase seen for CB5O.4. This was confirmed on the basis of a phase diagram constructed using binary mixtures of the two dimers that revealed complete miscibility across the complete composition range, see Figure S2. CB5O.t4 exhibits only a monotropic nematic phase.

CB6O.4 exhibits an enantiotropic nematic phase and a monotropic twist-bend nematic phase, and the local periodicity in both, as determined from the position of

the small-angle diffuse signal in their X-ray diffraction patterns, suggested a locally intercalated arrangement of the molecules [47]. Neither CB6O.s4 or CB6O.t4 exhibited liquid crystalline behaviour.

CB8O.4 shows five liquid crystalline phases, see Figure 8. On cooling from the isotropic liquid, a nematic phase develops which transforms on further cooling into a twist-bend nematic phase. At this transition there is a cessation of the optical flickering associated with director fluctuations in the nematic phase, and the schlieren texture becomes blocky, see Figure 8. This texture changes to give a focal conic fan texture, which may be sheared to give a schlieren texture containing predominantly two-brush point singularities suggesting that this is an anticlinic SmC_A phase. On cooling, this texture becomes brighter and smoother with the defect lines blurring, and at a lower temperature, scratches develop across the texture, see Figure 8. Similar changes were observed for members of the CT6O.m series [36], and by analogy we have

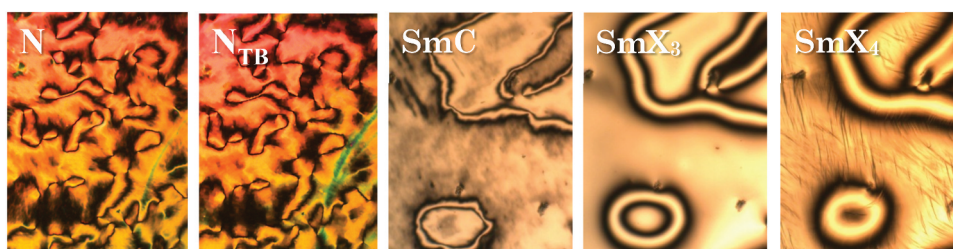


Figure 8. (Colour online) The textures obtained using the polarised optical microscope for CB80.4 in (from left to right) the nematic, the twist-bend nematic, the smectic C, the smectic X_3 and the soft crystal X_4 phases.

designated the higher temperature phase as a hexatic SmX_3 phase and the lower temperature phase as a soft-crystal X_4 phase. Nematic behaviour is extinguished for CB80.s4 and instead this compound undergoes a direct SmC_A -I transition. The schlieren texture is particularly temperature dependent suggesting strong changes of the tilt angle. These cease abruptly at the transition to the lower temperature phase, the schlieren texture blurs and regions of mosaic-like pattern develop. On further cooling, fracture-like defects develop and there is a subtle change in birefringence, see Figure S3. We have tentatively assigned these two lower temperature smectic phases to be the same as those shown by CB80.4, i.e. SmX_3 and X_4 , respectively. CB80.t4 does not exhibit liquid crystallinity.

CB100.4 shows very similar phase behaviour to that described for CB80.4, except that the stability of the SmC_A phase has increased such that a SmC_A -N transition is observed, see Figure S4 and the N_{TB} phase has been extinguished. CB100.s4, similarly as CB80.s4,

shows a I- SmC_A transition, and on cooling three additional smectic phases, see Figure S5. On cooling the SmC_A phase, a texture similar to that described for the SmX_3 phase shown by CB80.4 is obtained, see Figure S4. On cooling this, a texture consisting of partially transparent plates is obtained which persists until the formation of scratch-like defects resembling that seen for the SmX_4 phase described earlier for CB80.4. We suggest that CB100.s4 exhibits an additional phase, SmX_5 , intermediate between the SmX_3 and SmX_4 phases. CB100.t4 exhibits a monotropic SmC_A phase and further characterisation of this phase is precluded by the onset of rapid crystallisation.

Discussion

In all nine groups of materials listed in Tables 1 and 3, the *tert*-butyl homologues show the highest melting point, and in all but two, the butyl homologue has the lowest melting point. For the CBO110.X and CB100.X

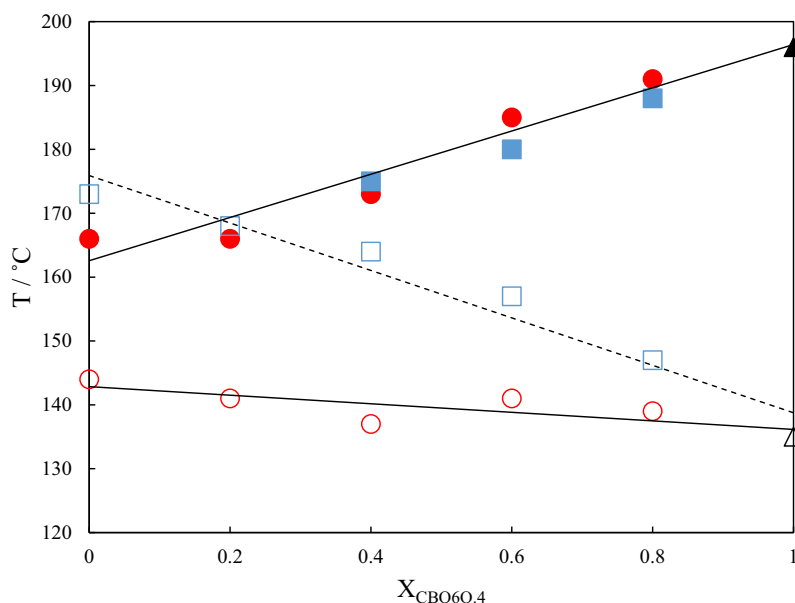


Figure 9. (Colour online) The dependence of the transition temperatures on the mole fraction of CBO60.4 for binary mixtures of CBO60.4 with CBO60.s4 (red circles) and with CBO60.t4 (blue squares). the triangles indicate the transition temperatures for CBO60.4. Filled symbols denote N-I transitions and open symbols either SmA -N or SmA -I transitions. Only Sm -N/I and N-I transitions are shown for the sake of clarity.

series, the melting points of the *sec*-butyl members are slightly lower than those of the corresponding butyl homologues. This implies that, in general, branching the terminal chain in these nonsymmetric dimers improves their packing efficiency within the crystalline structure and this is a theme we will return to later.

All the dimers containing a butyl terminal chain show a nematic-isotropic transition with the single exception of CBO12O.4, for which a smectic A-isotropic transition is observed. By comparison, only four of the *sec*-butyl substituted homologues show a nematic phase, namely, CB5O.s4, CBO4O.s4, CBO5O.s4 and CBO6O.s4, and of the *tert*-butyl substituted dimers, just CB5O.t4 exhibits a nematic phase. It is important to note that nematic behaviour is only observed for the branched chain homologues containing shorter spacers, and on increasing spacer chain length the branched terminal chain homologues become exclusively smectic in nature. The average reduction in the value of T_{NI} on exchanging a butyl chain for a *sec*-butyl one is around 40 K. In the only set of materials for which a comparison is possible, CB5O.X, the reduction in T_{NI} on replacing a *sec*-butyl by a *tert*-butyl group is 7 K. This reduction is considerably smaller than the decrease in T_{NI} of 37 K between CB5O.4 and CB5O.s4. Twist-bend nematic behaviour is not observed for any of these dimers containing a branched terminal chain, and this is in accord with the view that chain branching tends to destabilise the N_{TB} phase [46]. A very different pattern of behaviour emerges if we now compare the Sm-I transitions. The

only group for which all three dimers exhibit a SmA-I transition are the CBO12O.X dimers and the reduction in T_{SmAI} on moving from the butyl to *sec*-butyl chain is 17 K whereas replacing the *sec*-butyl chain by the *tert*-butyl chain actually increases T_{SmAI} by 6 K. Thus, the difference in T_{SmAI} between CBO12O.4 and CBO12O.t4 is only 9 K compared to the 44 K decrease in T_{NI} moving from CB5O.4 to CB5O.t4. Indeed, in each group of materials for which a smectic-isotropic transition is observed for both the *sec*- and *tert*-butyl substituted dimers, the latter show the higher clearing temperatures, on average by 9 K.

Conventional wisdom accounts for the reduction in the clearing temperature on branching a terminal chain in terms of the associated reduction in shape anisotropy, and, for a smectic-isotropic transition, the resulting reduction in the lateral intermolecular interactions. For these particular nonsymmetric dimers, we must take into account the potential disruption of the favourable unlike mesogenic unit interaction. Within this overarching framework, it is surprising that we do not see a larger reduction in T_{NI} on moving from CB5O.s4 to CB5O.t4. Even more surprising are the observations of a much smaller decrease in T_{SmAI} passing from CBO12O.4 to CBO12O.s4, and an increase on moving to CBO12O.t4.

To account for these observations, we must now consider the intercalated nature of the local molecular packing in both the nematic and smectic phases. We have seen that the formation of these intercalated smectic phases is thought to be driven by a specific favourable

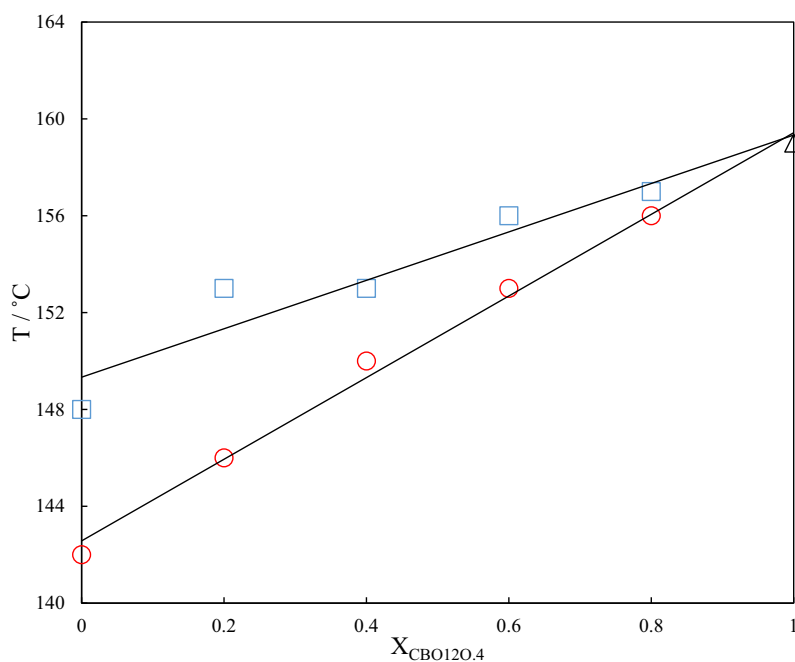


Figure 10. (Colour online) The dependence of the smectic A-isotropic transition temperatures, T_{SmAI} , on the mole fraction of CBO12O.4 for binary mixtures of CBO12O.4 with CBO12O.s4 (red circles) and with CBO12O.t4 (blue squares). The triangle indicates T_{SmAI} for CBO6O.4. Only SmA-I transitions are shown for the sake of clarity.

interaction between the unlike mesogenic units [1,2], and in such an arrangement, the terminal chains are accommodated in a volume governed by the length of the flexible spacer, see Figure 1. In all nine groups of dimers reported here, the terminal chains are shorter than the spacer and thus intercalated smectic behaviour is possible and indeed observed. For the shortest even-membered spacers, CB5O.X and CBO4O.X, smectic and nematic behaviour is seen for the butyl-substituted dimers and for CB5O.s4. In the nematic phase, the primary effect of chain branching is to reduce the shape anisotropy and disrupt the specific interaction between the unlike mesogenic groups. Both these effects serve to reduce T_{NI} . In the smectic phases, however, the shorter, branched terminal chain may fill the volume in the intercalated structure more efficiently and enhance the stability of the phase, and this accounts for the increase in the smectic-isotropic transition temperatures moving from a *sec*-butyl to a *tert*-butyl terminal chain for dimers having the longer spacers. This greater packing efficiency also accounts for the higher melting temperatures shown by the *tert*-butyl homologues.

The greater tendency for the *tert*-butyl group to promote smectic behaviour than the *sec*-butyl chain is evident in the behaviour of binary mixtures of each with the corresponding butyl terminated dimer. Figure 9 shows, for example, the transition temperatures of the binary mixtures of CBO6O.4 with the corresponding branched dimers. As the mole fraction of CBO6O.4 is reduced in both sets of mixtures, T_{NI} falls as would be expected. Surprisingly, however, the N-I trendline for both sets of mixtures is essentially identical indicating that the combined effect of the *sec* or *tert*-butyl chains in reducing the structural anisotropy and disrupting the intermolecular interactions compared to CBO6O.4 are more or less the same in the nematic phase. By comparison, however, the SmA-N/I trendline increases as the mole fraction of CBO6O.4 is reduced for both sets of mixtures, but now the two lines have very different gradients with that associated with the *tert*-butyl mixtures being much steeper. Indeed, the SmA-N trendline intersects the N-I trendline such that the 0.8 mole fraction CBO6O.t4 mixture shows a SmA-I transition, as does pure CBO6O.t4, whereas the corresponding *sec*-butyl mixture and CBO6O.s4 both show nematic phases over a temperature range of about 20 K. This enhanced stabilisation of the smectic A phase by the *tert*-butyl chain is further evident in the behaviour of binary mixtures of CBO12O.4 with the corresponding branched dimers, see Figure 10. All three CBO12O.X dimers exhibit a smectic A-isotropic transition. Addition of either CBO12O.s4 or CBO12O.t4 to CBO12O.4 decreases T_{SmAI} , but the reduction is larger for the *sec*-

butyl homologue. This further supports the view that the *tert*-butyl group can fill space more effectively in the intercalated structure.

Finally, it is interesting to note that the longer odd-membered dimers have a strong tendency to exhibit tilted intercalated phases, whereas their even-membered counterparts show orthogonal phases. This has been attributed to the difference in shape between odd- and even-membered dimers [31]. Specifically, the bent odd-membered dimers experience greater difficulty packing into an intercalated arrangement and this provides the driving force for the formation of the intercalated smectic C phase in which the tilt direction alternates between the layers such that globally the tilt angle is zero, but non-zero within a layer [31].

Conclusions

The very general observation is that in a low molar mass liquid crystal branching a terminal chain reduces the liquid crystal transition temperatures. For the nonsymmetric dimers reported here, this is indeed the case on comparing their values of T_{NI} . Thus, the value of T_{NI} falls by around 40 K on passing from the *n*-butyl to *sec*-butyl-substituted dimer. Somewhat surprisingly, for the only pair of dimers for which a comparison is possible, the decrease between the *sec*-butyl and *tert*-butyl homologues is just 7 K. By contrast, however, the *tert*-butyl homologues show higher values of T_{SmI} than their *sec*-butyl counterparts, and in the only direct comparison possible, the value of T_{SmAI} for *tert*-butyl dimers is only marginally lower than that of the corresponding *n*-butyl homologue. This highly surprising observation may be accounted for in terms of the intercalated structure of the smectic phases formed by these dimers, and specifically the better packing efficiency afforded by the *tert*-butyl group within this structure in which the ability to accommodate the branched terminal chain increases with spacer length.

Acknowledgements

EG and DP thank the National Science Centre (Poland) for financial support under the grant no. 2016/22/A/ST5/00319. RW gratefully acknowledges The Carnegie Trust for the Universities of Scotland for funding the award of a PhD scholarship 2015–2018

Disclosure statement

No potential conflict of interest was reported by the author(s).

Funding

The work was supported by the National Science Centre (Poland) [2016/22/A/ST5/00319].

ORCID

Rebecca Walker  <http://orcid.org/0000-0001-5167-7183>
 Damian Pocięcha  <http://orcid.org/0000-0001-7734-3181>
 Ewa Gorecka  <http://orcid.org/0000-0002-8076-5489>
 Corrie T. Imrie  <http://orcid.org/0000-0001-6497-5243>

References

- [1] Imrie CT, Henderson PA. Liquid crystal dimers and higher oligomers: between monomers and polymers. *Chem Soc Rev.* 2007;36(12):2096–2124.
- [2] Imrie CT, Henderson PA, Yeap GY. Liquid crystal oligomers: going beyond dimers. *Liq Cryst.* 2009;36(6–7):755–777.
- [3] Cestari M, Diez-Berart S, Dunmur DA, et al. Phase behavior and properties of the liquid-crystal dimer 1'',7''-bis(4-cyanobiphenyl-4'-yl) heptane: a twist-bend nematic liquid crystal. *Phys Rev E.* 2011;84(3):031704.
- [4] Henderson PA, Imrie CT. Methylene-Linked liquid crystal dimers and the twist-bend nematic phase. *Liq Cryst.* 2011;38(11–12):1407–1414.
- [5] Borshch V, Kim YK, Xiang J, et al. Nematic twist-bend phase with nanoscale modulation of molecular orientation. *Nat Commun.* 2013;4(1):2635.
- [6] Strachan GJ, Harrison WTA, Storey JMD, et al. Understanding the remarkable difference in liquid crystal behaviour between secondary and tertiary amides: the synthesis and characterisation of new benzanilide-based liquid crystal dimers. *Phys Chem Chem Phys.* 2021;23(22):12600–12611.
- [7] Walker R, Majewska M, Pocięcha D, et al. Twist-Bend nematic glasses: the synthesis and characterisation of pyrene-based nonsymmetric dimers. *Chemphyschem.* 2021;22:461–470.
- [8] Forsyth E, Paterson DA, Cruickshank E, et al. Liquid crystal dimers and the twist-bend nematic phase: on the role of spacers and terminal alkyl chains. *J Molec Liq.* 2020;320:114391.
- [9] Abberley JP, Walker R, Storey JMD, et al. Molecular structure and the twist-bend nematic phase: the role of terminal chains. *Liq Cryst.* 2020;47(8):1232–1245.
- [10] Walker R, Pocięcha D, Storey JMD, et al. The chiral twist-bend nematic phase (N*(TB)). *Chem Eur J.* 2019;25(58):13329–13335.
- [11] Cruickshank E, Salamonczyk M, Pocięcha D, et al. Sulfur-Linked cyanobiphenyl-based liquid crystal dimers and the twist-bend nematic phase. *Liq Cryst.* 2019;46(10):1595–1609.
- [12] Paterson DA, Walker R, Abberley JP, et al. Azobenzene-Based liquid crystal dimers and the twist-bend nematic phase. *Liq Cryst.* 2017;44:2060–2078.
- [13] Abberley JP, Storey JMD, Imrie CT. Structure-Property relationships in azobenzene-based twist-bend nematogens. *Liq Cryst.* 2019;46(13–14):2102–2114.
- [14] Mandle RJ. Designing liquid-crystalline oligomers to exhibit twist-bend modulated nematic phases. *Chem Rec.* 2018;18(9):1341–1349.
- [15] Lesac A, Baumeister U, Dokli I, et al. Geometric aspects influencing N-N-TB transition - implication of intra-molecular torsion. *Liq Cryst.* 2018;45(7):1101–1110.
- [16] Archbold CT, Andrews JL, Mandle RJ, et al. Effect of the linking unit on the twist-bend nematic phase in liquid crystal dimers: a comparative study of two homologous series of methylene- and ether-linked dimers. *Liq Cryst.* 2017;44:84–92.
- [17] Archbold CT, Mandle RJ, Andrews JL, et al. Conformational landscapes of bimesogenic compounds and their implications for the formation of modulated nematic phases. *Liq Cryst.* 2017;44:2079–2088.
- [18] Mandle RJ, Goodby JW. Dependence of mesomorphic behaviour of methylene-linked dimers and the stability of the N-TB/N-X phase upon choice of mesogenic units and terminal chain length. *Chem: Eur J.* 2016;22(27):9366–9374.
- [19] Knezevic A, Dokli I, Novak J, et al. Fluorinated twist-bend nematogens: the role of intermolecular interaction. *Liq Cryst.* 2021;48(5):756–766.
- [20] Knezevic A, Sapunar M, Buljan A, et al. Fine-Tuning the effect of π - π interactions on the stability of the N-TB phase. *Soft Matter.* 2018;14(42):8466–8474.
- [21] Ivsic T, Baumeister U, Dokli I, et al. Sensitivity of the N-TB phase formation to the molecular structure of imino-linked dimers. *Liq Cryst.* 2017;44:93–105.
- [22] Panov VP, Vij JK, Mehl GH. Twist-Bend nematic phase in cyanobiphenyls and difluoroterphenyls bimesogens. *Liq Cryst.* 2017;44:147–159.
- [23] Arakawa Y, Komatsu K, Inui S, et al. Thioether-Linked liquid crystal dimers and trimers: the twist-bend nematic phase. *J Molec Str.* 2020;1199:126913.
- [24] Arakawa Y, Komatsu K, Ishida Y, et al. Thioether-Linked azobenzene-based liquid crystal dimers exhibiting the twist-bend nematic phase over a wide temperature range. *Liq Cryst.* 2021;48(5):641–652.
- [25] Arakawa Y, Tsuji H. Selenium-Linked liquid crystal dimers for twist-bend nematogens. *J Molec Liq.* 2019;289:111097.
- [26] Abberley JP, Killah R, Walker R, et al. Heliconical smectic phases formed by achiral molecules. *Nat Commun.* 2018;9(1):228.
- [27] Salamonczyk M, Vaupotic N, Pocięcha D, et al. Multi-Level chirality in liquid crystals formed by achiral molecules. *Nat Commun.* 2019;10(1):1922.
- [28] Pocięcha D, Vaupotic N, Majewska M, et al. Photonic bandgap in achiral liquid crystals—A twist on a twist. *Adv Mater.* 2021;33(39):2103288.
- [29] Hogan JL, Imrie CT, Luckhurst GR. Asymmetric dimeric liquid crystals the preparation and properties of the α -(4-cyanobiphenyl-4'-oxy)- ω -(4-n-alkylanilinebenzylidene-4'-oxy)hexanes. *Liq Cryst.* 1988;3(5):645–650.
- [30] Attard GS, Garnett S, Hickman CG, et al. Asymmetric dimeric liquid-crystals with charge-transfer groups. *Liq Cryst.* 1990;7(4):495–508.

- [31] Attard GS, Date RW, Imrie CT, et al. Non-Symmetric dimeric liquid crystals the preparation and properties of the α -(4-cyanobiphenyl-4'-yloxy)- ω -(4-n-alkylanilinebenzylidene-4'-oxy)alkanes. *Liq Cryst.* **1994**;16(4):529–581.
- [32] Blatch AE, Fletcher ID, Luckhurst GR. The intercalated smectic a phase. the liquid crystal properties of the α -(4-cyanobiphenyl-4'-yloxy)- ω -(4-alkyloxycinnamate)alkanes. *Liq Cryst.* **1995**;18(5):801–809.
- [33] Walker R, Pocięcha D, Storey JMD, et al. Remarkable smectic phase behaviour in odd-membered liquid crystal dimers: the CT6O.M series. *J Mater Chem C.* **2021**;9(15):5167–5173.
- [34] Imrie CT, Henderson PA, Seddon JM. Non-Symmetric liquid crystal trimers. the first example of a triply-intercalated alternating smectic C phase. *J Mater Chem.* **2004**;14:2486–2488.
- [35] Donaldson T, Henderson PA, Achard MF, et al. Non-Symmetric chiral liquid crystal trimers. *Liq Cryst.* **2011**;38(10):1331–1339.
- [36] Donaldson T, Henderson PA, Achard MF, et al. Chiral liquid crystal tetramers. *J Mater Chem.* **2011**;21(29):10935–10941.
- [37] Knezevic A, Dokli I, Sapunar M, et al. Induced smectic phase in binary mixtures of twist-bend nematogens. *Beilstein J Nanotech.* **2018**;9:1297–1307.
- [38] Sepelj M, Lesac A, Baumeister U, et al. Intercalated liquid-crystalline phases formed by symmetric dimers with an α,ω -diiminoalkylene spacer. *J Mater Chem.* **2007**;17(12):1154–1165.
- [39] Pocock EE, Mandle RJ, Goodby JW. Experimental and computational study of a liquid crystalline dimesogen exhibiting nematic, twist-bend nematic, intercalated smectic, and soft crystalline mesophases. *Molecules.* **2021**;26(3):532.
- [40] Mandle RJ, Goodby JW. A twist-bend nematic to an intercalated, anticlinic, biaxial phase transition in liquid crystal bimesogens. *Soft Matter.* **2016**;12(5):1436–1443.
- [41] Mandle RJ, Goodby JW. Intercalated soft-crystalline mesophase exhibited by an unsymmetrical twist-bend nematogen. *Cryst Eng C omm.* **2016**;18(45):8794–8802.
- [42] Dawood AA, Grossel MC, Luckhurst GR, et al. On the twist-bend nematic phase formed directly from the isotropic phase. *Liq Cryst.* **2016**;43(1):2–12.
- [43] Dawood AA, Grossel MC, Luckhurst GR, et al. Twist-Bend nematics, liquid crystal dimers, structure-property relations. *Liq Cryst.* **2017**;44:106–126.
- [44] Paterson DA, Gao M, Kim YK, et al. Understanding the twist-bend nematic phase: the characterisation of 1-(4-cyanobiphenyl-4'-yloxy)-6-(4-cyanobiphenyl-4'-yl)hexane (CB6OCB) and comparison with CB7CB. *Soft Matter.* **2016**;12(32):6827–6840.
- [45] Paterson DA, Crawford CA, Pocięcha D, et al. The role of a terminal chain in promoting the twist-bend nematic phase: the synthesis and characterisation of the 1-(4-cyanobiphenyl-4'-yl)-6-(4-alkyloxyanilinebenzylidene-4'-oxy)hexanes. *Liq Cryst.* **2018**;45(13–15):2341–2351.
- [46] Abberley JP, Jansze SM, Walker R, et al. Structure-Property relationships in twist-bend nematogens: the influence of terminal groups. *Liq Cryst.* **2017**;44:68–83.
- [47] Walker R, Pocięcha D, Strachan G, et al. Molecular curvature, specific intermolecular interactions and the twist-bend nematic phase: the synthesis and characterisation of the 1-(4-cyanobiphenyl-4'-yl)-6-(4-alkylanilinebenzylidene-4'-oxy)hexanes (CB6O.m). *Soft Matter.* **2019**;15(15):3188–3197.
- [48] Yeap GY, Hng TC, Yeap SY, et al. Why do non-symmetric dimers intercalate? the synthesis and characterisation of the α -(4-benzylidene-substituted-aniline-4'-oxy)- ω -(2-methylbutyl-4'-(4''-phenyl)benzoateoxy)alkanes. *Liq Cryst.* **2009**;36(12):1431–1441.
- [49] Crivello JV, Deptolla M, Ringsdorf H. The synthesis and characterization of side-chain liquid crystal polymers based on polystyrene and poly- α -methystyrene. *Liq Cryst.* **1988**;3(2):235–247.